Proceedings of the 2007 American Control Conference
Marriott Marquis Hotel at Times Square
New York City, USA, July 11-13, 2007

Transient Force Atomic Force Microscopy: A New Nano-Interrogation Method

Deepak R. Sahoo, Pranav Agarwal and Murti V. Salapaka,
NanoDynamics and Systems Laboratory,
Department of Electrical and Computer Engineering,
Iowa State University, Ames, Iowa, USA, 50011.

***Abstract*— Atomic force microscopes (AFMs) are the primary investigation systems at the nanoscale. In existing dynamic mode AFM methods steady-state response of microcantilever is monitored for imaging tip-surface interaction forces at the nano-scale. In these methods microcantilevers with high quality factor are employed for high force sensitivity but at the cost of speed due to dependence on steady-state signals. In this paper, a novel methodology for fast interrogation of material that exploits the transient part of the cantilever response is presented. This method effectively addresses the perceived fundamental limitation on bandwidth due to high quality factors. Analysis and experiments show that the method results in significant increase in bandwidth and resolution as compared to the steady-state-based methods. This paper demonstrates the effectiveness of a systems perspective to the field of imaging at the nano-scale and for the first time reports real-time imaging at the nanoscale using the transient method with scan speed 40 times faster than conventional methods.**

I. INTRODUCTION

The atomic force microscope (AFM) [1] (see caption of Figure 1 for the operating principle) is a powerful tool to control, interrogate and manipulate matter at the atomic scale. Cantilevers in AFM have been utilized in biological sciences to perform remarkable feats such as cutting DNA strands [2] and investigating the activity of RNA polymerase [3].

The most prevalent mode of AFM operation is the dynamic mode, particularly when soft samples are to be imaged. In tapping-mode, which is the preferred mode of dynamic mode operation under ambient conditions, the base of the cantilever is forced sinusoidally using a dither piezo. The amplitude and phase of the cantilever oscillation change due to tip-sample interaction. In amplitude modulation (AM-AFM) method, the amplitude and phase of the first harmonic of the cantilever oscillation is obtained from the cantilever deflection signal. A set-point amplitude is regulated by applying feedback to z-scanner. In this scheme, the feedback signal forms the image of the sample. When low feedback gains are employed, which is essentially open-loop operation (also termed as error-signal-mode ESM-AFM), the amplitude and phase provide the image of the sample.

At present, however, the speed of operation of an AFM is much slower than the time resolution required to visualize real-time behavior of many macromolecular processes. Recently, three approaches to increase the throughput of an AFM were reported.

This work was supported by NSF grants CMS-0626171 and ECS-0601571.

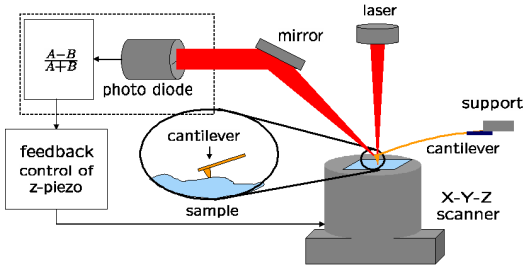

Fig. 1. A typical AFM setup with integrated xyz-scanner and photo-diode detector is shown. The main probe of an AFM is a micro-cantilever with a sharp tip at one end. The cantilever and the instrumentation is such that the deflection of the tip, due to interatomic forces between the tip atoms and the atoms on the sample, can be measured. In a typical AFM, the deflection of the cantilever due to the sample is registered by the laser incident on the cantilever tip, which reflects into a split photo-diode. Typically, a piezoelectric scanner is used to position the sample. The scanner is rastered in the lateral direction and the deflection of the tip is used to interpret sample properties. In the dynamic mode, the cantilever support is forced sinusoidally using a dither piezo. The sinusoidal forcing is typically at the first resonant frequency of the cantilever which induces a sinusoidal motion of the cantilever tip. The sinusoidal motion gets altered when the tip interacts with the sample. The alterations are registered and interpreted to derive sample topography or other sample properties.

One approach is to increase the mechanical bandwidth of AFM instrument by incorporating high-speed components. By integrating small (high resonant frequency) cantilever, high bandwidth electronics [4] and high-speed scanner, a scan speed of $\sim 600\mu$m/sec can be achieved [5] in tapping-mode-AFM. However, in this approach, imaging is limited to a small scan area $\sim 250\mu m \times 250\mu m$ due to the reduced size of AFM. By integrating the z-piezo actuator into the cantilever and reducing the quality factor of cantilever electronically (i.e. active Q-control), the bandwidth of AFM is further increased and a scan speed of 5 mm/sec can be achieved [6]. Unfortunately, this approach of increasing the mechanical bandwidth of AFM has not reached the speed for real-time video imaging of practical sized sample.

In the second approach [7] a micro-resonant scanner is used in open-loop for raster scanning in the fast axis direction which uses rather than avoiding the mechanical resonance that limits the speed of imaging using conventional scanners. However, the operation is not a dynamic mode method.

The third approach is to deploy a large array of cantilevers in parallel to increase the throughput of an AFM. Such an approach is taken in high density data storage devices to increase the data rates [8].

Most of the current dynamic mode approaches rely on the

steady-state part of the cantilever response for imaging. Due to the high quality factor of the cantilever the settling time is high. Also, high quality factor is required for high resolution. Therefore, existing techniques are limited to slow scan speeds due to tradeoff between bandwidth and resolution. In steady state based methods, therefore, there is a fundamental limitation on the bandwidth of operation.

The authors have pioneered a new mode of interrogation at the nanoscale that introduces systems concepts to the area of AFM based imaging. In [9] and [10] the authors reported that an observer based methodology can lead to ultrafast detection of the sample where detection at rates two orders faster was reported. These results infer the sample presence or absence based on the cantilever deflection. The observer based methods made it possible to obtain sample detection results even when the cantilever is in the transient part and has not reached its steady state. In this paper, the hitherto unexplored idea of transient force atomic microscopy (TF-AFM) that uses the transient part of cantilever response for *imaging* is reported. With the results reported in this paper, it is evident that TF-AFM can be used to image samples like DNA, that have small feature size, 40 times faster than the conventional speeds. It is to be noted that DNA samples due to their small feature size (approximately 1-2 nm in height) are particularly challenging to image, thus reinforcing the high resolution feature of TF-AFM. This paper can also be viewed as a culmination of an entire body of work where tools from system theory as developed in [9] and [10] together with the imaging results presented in this paper provide definitive evidence to the efficacy of systems based approach.

The paper is organized as follows. In Section II, the state-space description of the cantilever dynamics is introduced and the observer architecture is described that provides the vital transient signal. Active Q-control is introduced to this method in Section III which seamlessly integrates without affecting the transient signals. Assumptions on the nature of tip-sample interactions is introduced in Section IV to characterize transient signals. Bandwidth and signal to noise ratio concerns are addressed in Section V. Moreover, efficient detection and imaging algorithms are developed in Section VI using tools from statistical signal processing. Experimental results are presented in Section VII that demonstrates the effectiveness of transient force atomic force microscopy (TF-AFM).

II. Cantilever-Observer Architecture

A multi-mode model of cantilever can be precisely identified using its thermal noise response [11]. In this paper, we consider a model of AFM derived from its frequency response between dither input and photo-diode output. The transfer function fitting the frequency response data usually has a significant right-half-plane zero. State-space representation of AFM model is given by,

$$\begin{aligned} \dot{\overline{x}} &= A\overline{x} + B(w+\eta), \\ y &= C\overline{x} + \upsilon, \end{aligned} \tag{1}$$

where w, y, η and υ are external force applied to the cantilever, photo-diode signal, thermal noise and measurement noise, respectively. $\overline{x}$ is the state vector that contains cantilever tip-position and velocity.

In the systems viewpoint the cantilever dynamics is separated as an independent system from the sample subsystem that affects the cantilever in a feedback manner. This systems perspective of the AFM (see Figure 2) facilitates the design of an observer that provides an estimate $\hat{\overline{x}}$ of the state $\overline{x}$.

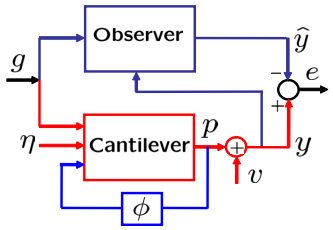

Fig. 2. In the systems perspective, the AFM dynamics is viewed as an interconnection of a linear cantilever system with the nonlinear tip-sample interaction forces in feedback. ϕ models the tip-sample interaction force that depends on the tip deflection p. The error process is denoted by e which is the actual deflection signal minus the estimated deflection signal.

The observer dynamics is given by,

$$\begin{aligned} \dot{\hat{\overline{x}}} &= A\hat{\overline{x}} + Bg + L(y-\hat{y}); \hat{\overline{x}}(0) = \hat{\overline{x}}_0, \\ \hat{y} &= C\hat{\overline{x}}, \end{aligned} \tag{2}$$

where $\hat{\overline{x}}$ is the estimate of the state $\overline{x}$ and g is the input applied to the dither piezo. The error in estimation of state is $\tilde{\overline{x}} = \overline{x} - \hat{\overline{x}}$. The error dynamics is given by,

$$\dot{\tilde{\overline{x}}} = (A-LC)\tilde{\overline{x}} + B(\phi+\eta) - L\upsilon; \tilde{\overline{x}}(0) = \overline{x}_0 - \hat{\overline{x}}_0. \tag{3}$$

The error in the estimate of the output y is given by,

$$e = y - \hat{y} = C\tilde{\overline{x}} + \upsilon. \tag{4}$$

It is evident that if the observer gain L is chosen so that the eigenvalues of the matrix $(A-LC)$ are in the strict left half complex plane, the state error $\tilde{x}$ due to the initial condition mismatch $\tilde{x}(0)$ goes to zero with time. The system is observable and therefore the eigenvalues of $(A-LC)$ can be placed anywhere. It can be shown that under the presence of the noise η and υ, the error process e approaches a zero mean wide sense stationary stochastic process when $\phi = 0$. When ϕ appears due to tip-sample interaction force, error e loses its zero mean wide sense stationary nature. Therefore error process is a good measure of the transients due to tip-sample interaction force on the cantilever.

There is considerable freedom on how fast the observer tracks the cantilever dynamics and consequently how long the effect of tip-sample interaction persists in error signal e. Note that high quality factors are detrimental to high bandwidth in steady state methods; however it is required for high resolution. *By utilizing the observer based architecture presented in this paper a method for effectively isolating the high bandwidth needs from the high resolution needs is obtained.*

III. Active Q-control

In AFM quality factor of cantilever Q is increased electronically to increase force sensitivity in order to image with

smaller force on the sample. Q is decreased to increase scan speed. The observer provides an estimate of the cantilever tip-velocity which can be used for active Q-control [12]. Thus Q-control comes naturally integrated into TF-AFM. In active Q-control, estimated velocity signal multiplied with state feedback gain F is added to standard dither signal g_1 and resultant signal $g = g_1 + F\hat{x}$ is given to the cantilever and the observer. It can be shown that (refer [12]) F does not affect the effective resonant frequency of the cantilever and changes only the effective Q of the cantilever. Also the transfer function from dither input to photo-diode output is of second order which is equivalent to the unaltered spring-mass-damper system with a different damping coefficient. From Equation(3) it can be shown that error signal e is independent of feedback gain F and is given by Equation(4). This facilitates analysis of TF-AFM independent of active Q-control.

IV. Tip-Sample Impact Model

The error profile e due to a tip-sample interaction can be better characterized if a model for the effect of the tip-sample interaction force on the cantilever-motion is available. We assume that the sample's influence on the cantilever tip is approximated by an impact condition where the position and velocity of the cantilever tip instantaneously assume a new value (equivalent to a state-jump). This is satisfied in most typical operations because in the dynamic mode, the time spent by the tip under the sample's influence is negligible compared to the time it spends outside the sample's influence. The assumption is also corroborated by experimental results [9].

V. Bandwidth and Signal to Noise Ratio

It can be shown that bandwidth B of signal e is given by the real parts of eigenvalues of the matrix $A-LC$. Since the choice of the observer gain L is independent of the quality factor Q, bandwidth of TF-AFM is effectively decoupled from quality factor of cantilever.

Signal to noise ratio (SNR) can be calculated from Equation(3) as a function of observer gain L. It can be shown that SNR due to thermal noise SNR_η improves if observer gain L is large [10]. This is because when the observer is more aggressive, it also tries to track the thermal noise response of the cantilever and thus reduces thermal noise contribution in error e. It can be shown that SNR due to measurement noise SNR_υ and consequently overall SNR degrades if observer gain L is large [10]. This is because the strength of signal due to state-jump ν reduces due to better tracking by the observer and the noise power due to measurement noise υ practically does not change with large L. Therefore gain L can not be chosen to be arbitrarily large. The bandwidth constraint is mainly imposed by the measurement noise. It is evident that a desired tradeoff between SNR and bandwidth can be obtained by an appropriate choice of L that is independent of Q. This provides considerable flexibility when compared to existing steady state methods where Q determines the bandwidth. Note that due to the small measurement noise, the observer gain L can be chosen large enough so that the cantilever state is tracked within a couple of cycles of the dither forcing. Therefore the optimal bandwidth is primarily dictated by the resonant frequency ω_0 of the cantilever.

VI. TF-AFM Algorithms

With the assumption of the state-jump condition, the effect of tip-sample force on error e can be formulated. A discretized model of the cantilever is given by,

$$\begin{aligned} x_{k+1} &= Fx_k + G(g_k + \eta_k) + \delta_{\theta,k+1}\nu, \\ y_k &= Hx_k + v_k,\ k \geq 0, \end{aligned} \tag{5}$$

where matrices F, G, and H are obtained from the continuous time model described by Equation(1).$\delta_{i,j} = 1$ if $i = j$ and $\delta_{i,j} = 0$ if $i \neq j$. θ denotes the time instant when the tip-sample interaction occurs and ν signifies the state-jump during the impact.

The thermal noise η and measurement noise υ are assumed to be white and uncorrelated. When an optimal observer i.e. the Kalman filter [13] is employed the error e is known as the *innovation* signal. e is a zero mean white process when tip-sample interaction forcing $\phi = 0$.

The innovation sequence $\{e_k\}$ can be written as,

$$\begin{aligned} e_k &= \Upsilon_{k;\theta}\nu + \gamma_k, \\ \Upsilon_{k;\theta} &= H(F - L_K H)^{k-\theta}, \end{aligned} \tag{6}$$

where $\{\Upsilon_{k;\theta}\nu\}$ is a known dynamic profile with unknown arrival time θ and magnitude ν. $\{\gamma_k\}$ is the white noise component in $\{e_k\}$ [14] and L_K is the steady state Kalman observer gain.

1) TF-AFM detection algorithm: TF-AFM based sample-detection scheme relies on detection of dynamic profile Υ in innovation sequence $\{e_k\}$. This problem is formulated in the framework of binary hypothesis testing (H_0 versus H_1) given by,

$$\begin{aligned} H_0 &: e_k = \gamma_k,\ k = 1, 2, \ldots, M \\ H_1 &: e_k = \Upsilon_{k;\theta}\ \nu + \gamma_k,\ k = 1, 2, \ldots, M \end{aligned}$$

where innovation sequence $\{e_k\}$ is windowed into M samples for detecting dynamic profile Υ.

To select between the two hypotheses, a likelihood ratio test is computed as [15],

$$l(M) = \frac{\overline{e}^T\overline{s}^T}{V} = \frac{\overline{e}^T\Upsilon}{V}(\frac{\Upsilon^T\Upsilon}{V})^{-1}\frac{\Upsilon^T\overline{e}}{V}, \tag{7}$$

where $\overline{e} = [e_1, e_2, \cdots, e_M]^T$, $\Upsilon = [H, H(F - L_K H), \cdots, H(F - L_K H)^{M-1}]^T$ and $E\{\gamma_j\gamma_k^T\} = V\delta_{ij}$. The likelihood ratio $l(M)$ is compared with a threshold value ϵ as $l(M) \gtrless_{H_0}^{H_1} \epsilon$ to arrive at a decision whether the dynamic profile is present or not (which is equivalent to detecting tip-sample interaction). The threshold ϵ is chosen so that false alarm rate P_F is small and detection probability P_D is high [10].

2) TF-AFM imaging algorithm: For real-time implementation TF-AFM based imaging the likelihood ratio calculation is currently simplified as a true-power detection algorithm given by,

$$r(M) = \frac{\overline{e}^T\overline{e}^T}{V}. \tag{8}$$

Though true-power of innovation signal is at least one order less sensitive than likelihood ratio, it is easy to implement and gives high quality imaging results for practical samples.

VII. Experimental Results

TF-AFM based high-speed and high-resolution detection of sample [10] is briefly revisited in the first subsection. TF-AFM based high-speed imaging of DNA sample is presented next.

A. High Speed Detection of Sample

In the following experiment a multi-mode AFM (from Digital Instruments), a freshly cleaved graphite (HOPG) sample, and a cantilever with resonant frequency $f_0 = 60.25$ kHz and quality factor $Q = 104$ were used.

Thermal and measurement noise powers were obtained experimentally from the photo-diode signal when the cantilever was freely oscillating in air and when it was held stiff against graphite surface. The cantilever was tuned to its resonant frequency and brought close to the sample. A 1 kHz and 1 V_{p-p} signal was applied to the z-scanner which generated a sample profile with 4 peaks separated by $\approx 100\ \mu s$ with average width and height of each peak $\approx 25\mu$s and ≈ 20 nm, respectively.

The sample profile, deflection signal, innovation signals (Innov I and II) from 2^{nd} and 4^{th} order Kalman observers, respectively and likelihood ratios (LHR I and II) calculated based on 2^{nd} order cantilever model are plotted in Figure 3. The 4 peaks in the sample profile are detected in the likelihood ratios using a threshold that can detect a 0.25 nm peak in the sample profile with 99% detection probability and 1% false alarm rate. Therefore a 2^{nd} order implementation of observer is sufficient for high-speed and high-resolution detection of sample. Note that 2^{nd} mode oscillations of the cantilever are present in Innov I and 2^{nd} mode dynamic profiles are seen in Innov II. The time-scale of tip-sample interaction implies that the cantilever is in transient state through out the experiment. This experiment demonstrates a sample detection rate of 10 kHz (equivalent to 10 kbits per second) using a 60.25 kHz cantilever. Assuming the dynamic profiles can be captured and detected within 4 cycles of cantilever oscillation, the achievable detection bandwidth is $\frac{f_0}{4}$ using a cantilever with resonant frequency f_0. Note that use of steady state signals limits detection bandwidth to $\frac{f_0}{Q}$ where Q is in the range of 100-200.

B. High Speed Imaging of DNA

1) Sample preparation: 500μg/ml Lambda DNA solution (Promega Corp. # D1501) was diluted to 50μg/ml concentration using Tris/HCl/EDTA buffer (10mM Tris/HCl, 1mM EDTA, pH 6.6-6.8). This solution was used as the stock solution. Working solution was prepared by further diluting to 1μg/ml concentration using $NiCl_2$ buffer (40mM HEPES, 5mM $NiCl_2$, pH 6.6-6.8). For imaging in air 20μl of working solution was incubated on a freshly cleaved mica surface for 10 minutes, and then rinsed with pure water and dried using nitrogen gas.

2) Experimental Setup: TF-AFM requires a commercial AFM and an electronic add-on that implements the observer (see Figure 4). In the current setup the observer is implemented on a FPGA (Xilinx Virtex 2-Pro XV30). The innovation signal from FPGA is fed to a true power detector circuit (Analog Devices AD8361) and the output is connected to the auxiliary input of AFM setup. TF-AFM

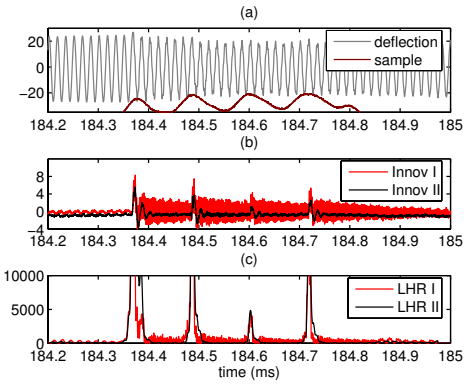

Fig. 3. (a) Cantilever deflection is plotted above sample position. (b) Innovation signals 'Innov I' from 2^{nd} order analog Kalman filter and 'Innov II' from 4^{th} order Kalman filer is plotted. (c) The likelihood ratios 'LHR I' and 'LHR II' calculated from 'Innov I' and 'Innov II' using 1^{st} mode dynamic profiles are plotted.

and AM-AFM images are then captured in parallel using existing AFM software. For active Q-control, the velocity estimate signal from the digital observer on FPGA is added to the standard dither signal and applied to the cantilever.

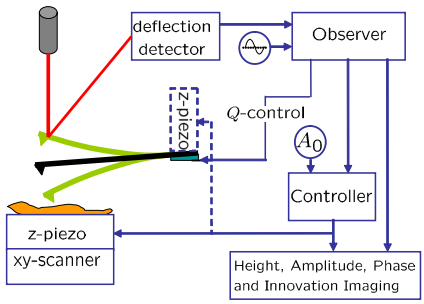

Fig. 4. A typical TF-AFM setup is shown. The amplitude A of the deflection signal of the cantilever is controlled at a set point amplitude of A_0 by actuating the z-piezo in a feedback manner. Velocity estimate signal from observer is used for Q-control. Control, amplitude and phase signals from AFM controller and innovation signal from observer give the height, amplitude, phase and TF-AFM images.

AM-AFM height image of Λ-DNA captured at scan-speed of 4 μm/sec is shown in Figure 5(a). The average height of DNA in the image is 1.5 nm. Typically DNA images are taken at lower scan speeds. Note that there are small specs present on the mica sample along with the long DNA strand with similar height feature. This image is taken as the reference image to compare with TF-AFM images.

TF-AFM needs tuning of scan parameters like set point amplitude, scan size and feedback gains to capture high quality images. In high-speed imaging right selection of scan parameters can reduce wear and tear of tip and sample significantly. Scan parameters tuned for AM-AFM imaging could be different from parameters chosen for high-speed TF-AFM imaging.

In the experiment, first the set point amplitude of cantilever was kept close to free oscillation amplitude. Then it was slowly reduced until images appeared. Z-piezo feedback gains after tuning were integral gain $k_i = 0.5$ and proportional gain $k_p = 1$. The scan speed was slowly increased

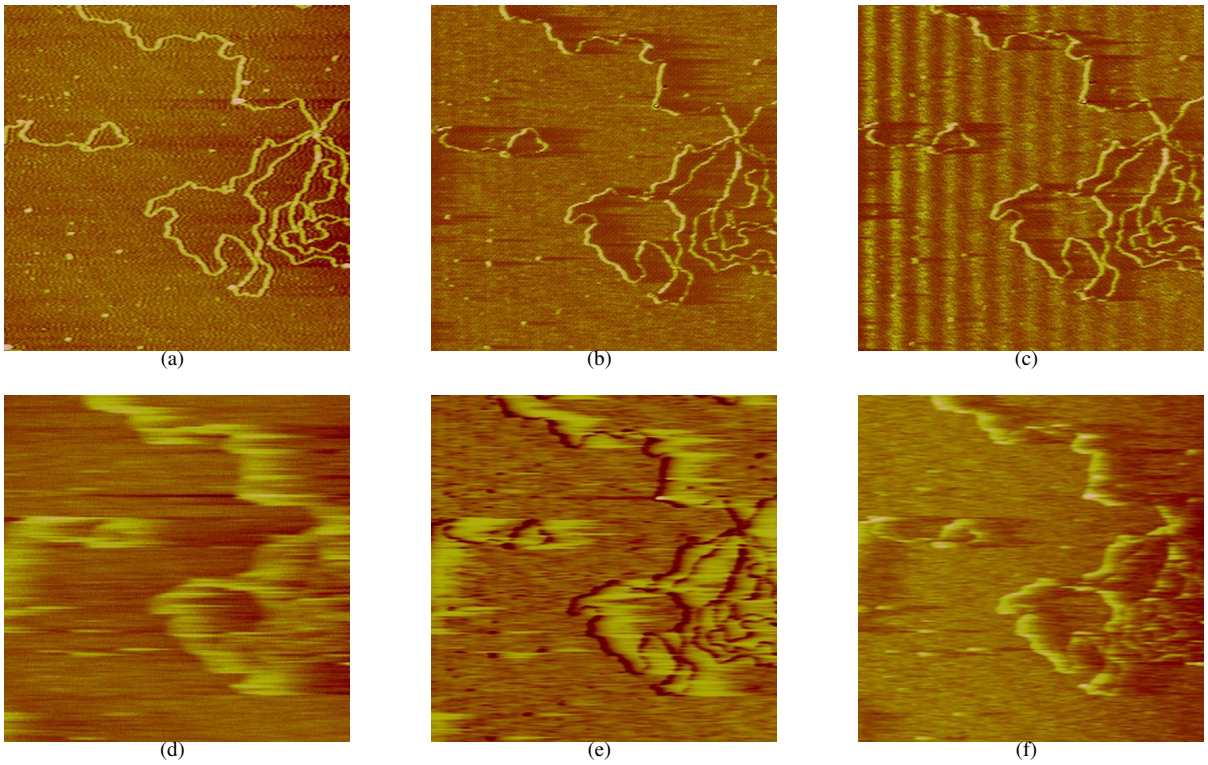

Fig. 5. (a) Height image taken at 4μm/sec, (d)height, (e) amplitude, (f) phase images taken at 97.68μm/sec and TF-AFM images taken at (b) 97.68μm/sec and (c) 162.8μm/sec of Lambda DNA are shown. Scan size $= 2\mu$m.

in steps and corresponding height, amplitude, phase and TF-AFM images were collected.

DNA height, phase, amplitude and TF-AFM images collected at scan speed of 97.68μm/sec are plotted in Figure 5(d),(e),(f) and (b), respectively. Compared to reference height image shown in Figure 5(a), the height image at 97.68μm/sec is very blurred. This can be attributed to small closed-loop bandwidth of AFM setup and fast varying spatial profile of DNA. The phase and amplitude images are also blurred. This can be attributed to the high quality factor of cantilever. However, the TF-AFM image at 97.68μm/sec shown in Figure 5(b) provides a high quality image of DNA and corresponds well to the reference image shown in Figure 5(a). The TF-AFM image distinctively captures the small specs on the sample in spite of high speed.

The scan speed was further increased to 162.8 μm/sec. In the process the quality of height, phase and amplitude images detoriated further due to small closed-loop bandwidth and high quality factor. However, TF-AFM image shown in Figure 5(c) still captures the DNA and the small specs distinctively. The vertical streaks in the images are due to resonant oscillations in the scanners since they are not suitable for high-speed experiments. During raster scanning, when the fast-axis x-scanner takes the sharp turn at the edge of the scan area, it rings which is coupled to z-scanner creating artificial sample features. Designs and methods to eliminate such artifacts during high-speed scanning are being investigated by the authors.

The effect of active Q-control on TF-AFM is investigated in the next experiment.

In this experiment, MFP3D AFM (from Asylum Research) and Plasmid DNA (pUC19 from Bayou Biolabs) are used. TF-AFM images of dna sample are captured in air with various scan parameters and active Q-control. In Figure 6 (a),(b) and (c) TF-AFM images taken at scan-speed of 97.655 μm/sec under active Q-control are shown for $Q = 155$ (nominal), $Q = 198$ and $Q = 104$, respectively. Spatial contrast in the TF-AFM images remained same for different values of Q. This can be attributed to the fact that TF-AFM is largely independent of quality factor of the cantilever [9]. When Q was actively increased from 155 to 198, the image looked neater with less background noise because the cantilever was interacting mildly with the sample surface giving rise to less transient signals. When Q was actively decreased from 155 to 104, the cantilever was interacting relatively harsher with the sample surface giving rise to more transient signals and correspondingly more background noise in the image. Due to larger tip-sample force DNA is distorted in several parts of the image in Figure 6(c) when Q was decreased. It can be concluded that TF-AFM imaging with active Q-increase is suitable for imaging soft biological samples as it provides high-speed and high-quality images while being softer on the sample.

VIII. Conclusion

Current AFM schemes utilize the steady-state part of cantilever response. TF-AFM has been an effort to exploit the transient-state part of cantilever response in order to develop an ultra-fast sample interrogation method. This paper summarizes TF-AFM and presents high-speed, high-resolution

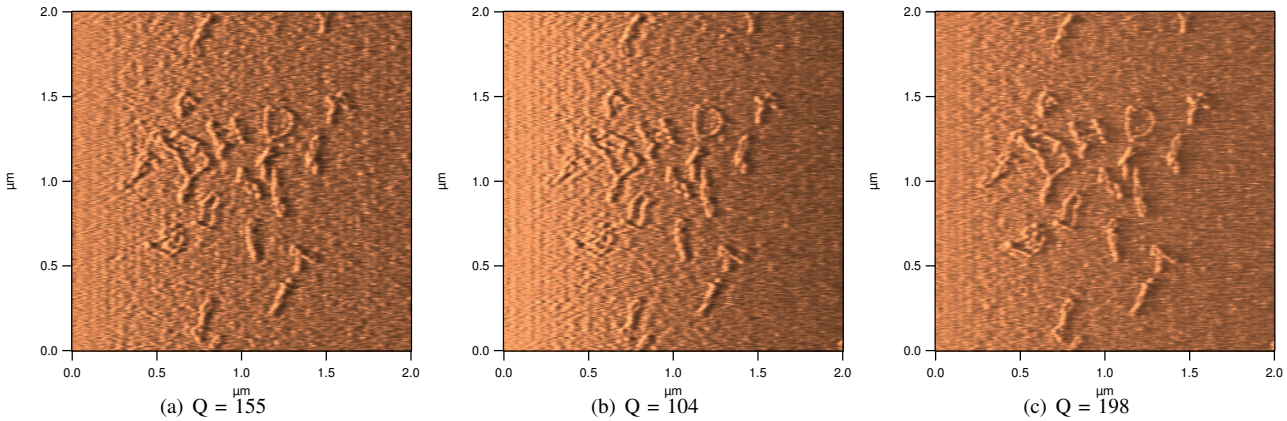

(a) Q = 155 (b) Q = 104 (c) Q = 198

Fig. 6. TF-AFM images of plasmid DNA captured at scan speed of 97.655μm/sec when the quality factor cantilever is changed from (a) $Q = 155$ to (b) $Q = 104$ and (c) $Q = 198$ using active Q-control.

sample-imaging results culminated from previous work.

In this paper a model based framework for high-speed and high-resolution imaging is presented. The cantilever and its interaction with the sample are modeled. A first mode approximation model of the AFM is considered and Kalman observers are designed to estimate the dynamic states. The tip-sample interaction is modeled as an impulsive force applied to the cantilever. The dynamics due to tip-sample interaction is characterized in the innovation signal and a likelihood ratio test is developed. The innovation signal provides the bandwidth and the likelihood ratio provides the resolution improvement. In a simplified version power of innovation signal is used for TF-AFM imaging.

A sample-detection bandwidth of $\frac{f_0}{4}$ can be achieved using a cantilever with resonant frequency f_0. In experiments using a 1^{st} mode analog observer a detection bandwidth of 10 kHz is demonstrated using a cantilever of resonant frequency $f_0 = 60.25$ kHz.

TF-AFM seamlessly integrates into commercial AFMs and high-speed TF-AFM images are captured along with AM-AFM images. TF-AFM requires an electronic add-on i.e. a digital observer and a true power detector. The high-speed and high-resolution imaging capabilities of TF-AFM is demonstrated by imaging DNA with 1.5 nm height at a scan speed of 162.8μm/sec which is more than 40 times faster than typical scan speeds. TF-AFM integrates active Q-control by using the estimated tip-velocity signal from the observer. Experiments show that spatial contrast in TF-AFM images is independent of quality factor. However, when the quality factor of the cantilever is increased, the background noise in the image is less and better TF-AFM images are obtained .

The systems perspective has facilitated the development of TF-AFM. In this methodology a perceived limitation in improving both resolution and bandwidth of imaging is effectively addressed using tools from signals and systems. This body of work, thus opens a new methodology for imaging at the nanoscale; that of imaging using models of known information employed in a real-time manner.

REFERENCES

[1] G. Binnig, C. Quate, and C. Gerber, "Atomic force microscope," *Physical Review Letters*, vol. 56, no.9, pp. pp. 930–3., 1986.

[2] J. H. Hoh, R. Lal, S. A. John, J. P. Revel, *et al.*, "Atomic force microscopy and dissection of gap junctions," *Science*, vol. 253, pp. 1405–1408, 1991.

[3] S. Kasas, N. H. Thomson, B. L. Smith, H. G. Hansma, and others., "Escherichia coli rna polymerase activity observed using atomic force microscopy," *Biochemistry*, vol. 36(3), pp. 461–468, 1997.

[4] D. A. Walters, J. P. Cleveland, N. H. Thomson, P. K. Hansma, M. A. Wendman, G. Gurley, and V. Elings, "Short cantilevers for atomic force microscopy," *Review of Scientific Instruments*, vol. 67, pp. 3583–3590, 1996.

[5] T. Ando, N. Kodera, E. Takai, D. Maruyama, K. Saito, and A. Toda, "A high-speed atomic force microscope for studying biological macromolecles," *Proceedings of the national Academy of Sciences of United States of America*, vol. 98, no. 22, pp. 12 468–12 472, 2001.

[6] T. Sulchek, R. Hsieh, J. Adams, G. Yaralioglu, S. Minne, C. Quate, J. Cleveland, A. Atalar, and D. Adderton, "High-speed tapping mode imaging with active q control for atomic force microscopy," *Applied Physics Letters*, vol. 76, no. 11, p. 1473, 2000.

[7] A. D. L. Humphris, M. J. Miles, and J. K. Hobbs, "A mechanical microscope: High-speed atomic force microscopy," *Applied Physics Letters*, vol. 86, p. 034106, 2005.

[8] P. Vettiger, G. Cross, M. Despont, U. Drechsler, U. Durig, B. Gotsman, W. Heberle, M. A. Lantz, H. E. Rothuizen, R. Stutz, and G. K. Binnig, "The "millipede" - nanotechnology entering data storage," *IEEE Transactions on Nanotechnology*, vol. 1, no. 1, pp. 39–55, 2002.

[9] D. R. Sahoo, A. Sebastian, and M. V. Salapaka, "Transient-signal-based sample-detection in atomic force microscopy," *Applied Physics Letters*, vol. 83(26), pp. 5521–5523, December 29,2003.

[10] ——, "Harnessing the transient signals in atomic force microscopy," *International Journal of Robust and Nonlinear Control*, vol. 15, pp. 805–820, 2005.

[11] M. V. Salapaka, H. S. Bergh, J. Lai, A. Majumdar, and E. McFarland, "Multimode noise analysis of cantilevers for scanning probe microscopy," *Journal of Applied Physics*, vol. 81(6), pp. 2480–2487, 1997.

[12] D. R. Sahoo, T. De, and M. V. Salapaka, "Observer based imaging methods for atomic force microscopy," *Proceedings of 44th IEEE Conference on Decision and Control*, pp. 1185–1190, December 12-15,2005.

[13] A. H. S. Thomas Kailath and B. Hassibi, "Linear Estimation," *Prentice Hall, NJ*, 2000.

[14] A. S. Willsky and H. L. Jones, "A Generalized Likelihood Ratio Approach to the Detection and Estimation of Jumps in Linear Systems," *IEEE Transactions on Automatic Control, pp. 108-112*, Feb. 1976.

[15] S. M. Kay, "Fundamentals of Statistical Signal Processing, Detection Theory, vol.II," *Prentice Hall, PTR*, 1993.